Design and Implementation of an Underlay Control Channel for NC-OFDM-Based Networks

Ratnesh Kumbhkar*, Gokul Sridharan*, Narayan B. Mandayam*, Ivan Seskar* and Sastry Kompella†
*WINLAB, Rutgers, The State University of New Jersey, North Brunswick, NJ, USA.
Email: {ratnesh, gokul, narayan, seskar}@winlab.rutgers.edu
†Information Technology Division, Naval Research Laboratory, Washington DC, USA
Email: sk@ieee.org

***Abstract*—This paper designs an underlay control channel for noncontiguous-OFDM-based cognitive networks. Noncontiguous OFDM (NC-OFDM) provides a fast and flexible manner of accessing disjoint parts of the spectrum and is ideally suited for dynamic spectrum access. While similar to OFDM, NC-OFDM explicitly restricts transmission to only certain subcarriers that are free of incumbent transmissions. In particular, this paper considers designing a control channel for a cognitive network consisting of multiple point-to-point (p2p) links that operate over a wide bandwidth that might encompass some primary transmissions. In such a scenario, control channel becomes vital not only to share basic transmission parameters but also to aid timing and frequency recovery of NC-OFDM transmission; a nontrivial problem in itself. The proposed design is a low-power underlay transmission that spans the entire bandwidth regardless of any incumbent transmissions and uses direct sequence spread spectrum (DSSS). The control channel operates in one of two modes. The first mode aids timing and frequency recovery through a two-step process, while the second mode is used for control data transmission. To enable multiple access, the p2p links use orthogonal pseudo-noise (PN) sequences. The proposed control channel is implemented on USRPs in the ORBIT testbed using GNU Radio. Experimental results suggest robust timing and frequency offset recovery even in the presence of concurrent primary transmissions and support for about 10 to 20kbps over a 1 MHz bandwidth at an uncoded symbol-error-rate of about 10^{-2} under typical operating conditions.**

***Keywords*—noncontiguous-OFDM, control channel design, frequency offset estimation, timing recovery, PN sequences.**

I. Introduction

With the ever increasing requirement for higher wireless data rates, efficient usage of all available spectrum, licensed or otherwise, becomes paramount. In particular, with the wide availability of unlicensed spectrum in the TV-white-space band, the U-NII and ISM bands, and the requirement for dynamic frequency selection (DFS) to avoid interference to radar or other ISM devices, the ability to effectively use noncontiguous spectrum is vital to exploit the full potential of the available spectrum. Cognitive radios (CRs) enabled with noncontiguous-OFDM (NC-OFDM) [1]–[4] are ideally suited to operate under such conditions as they permit dynamic spectrum access even when the available spectrum is fragmented. NC-OFDM is similar to OFDM, except that transmission on certain subcarriers is not permitted depending on the availability of the corresponding spectrum. In this context, this paper considers the design of a cognitive network of multiple point-to-point (p2p) links that operate over a wide bandwidth of several disjoint bands of frequencies, as shown in Fig. 1. Two key components to any cognitive network are the data plane and the control plane. Rather than treating them as two independent components, this paper takes a holistic approach and focuses on the design of a control channel that is tailor-made for an NC-OFDM-based data plane. In particular, we discuss the design and implementation of a low-power CDMA-like underlay control channel (UCC) for each link that is designed specifically with the needs of NC-OFDM in mind.

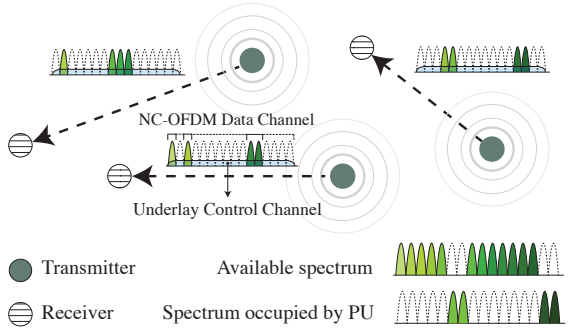

Fig. 1. A cognitive network of multiple point-to-point links using NC-OFDM to access noncontiguous spectrum.

Control channel design for cognitive networks is a well studied subject [5]–[12] with designs that can be broadly classified as either being in-band or out-of-band. Out-of-band designs call for a dedicated narrowband channel that is used to transmit the control signals [5], [8], while in-band designs typically involve a UCC spanning the full bandwidth [6], [7], [12]. While a dedicated narrowband control channel is straightforward to implement and provides higher reliability, setting aside a dedicated narrowband chunk of spectrum may not always be feasible, or sometimes even unnecessary. In-band designs typically propose to use spread spectrum techniques to implement a low-power UCC spanning the entire bandwidth with or without considerations for the primary transmissions [6], [7]. Although such a design is exposed to the primary and secondary transmissions, it involves no spectrum overhead and is well-suited for a low-data-rate communication channel. This paper proposes an in-band UCC spanning the entire bandwidth, as shown in Fig. 1.

Although NC-OFDM is similar to OFDM, there are significant challenges that emerge when using NC-OFDM in the presence of concurrent transmissions [13]–[18], with timing (to identify the start of an NC-OFDM frame) and frequency offset recovery being one among them. When a p2p cognitive link

uses NC-OFDM, the receiver of this link sees the aggregate of the desired NC-OFDM signal along with all the other concurrent transmissions. Due to the dynamic nature of this interference, it is not always possible to filter these transmissions out. Under such circumstances, traditional techniques for OFDM timing recovery that rely on some form of symmetry in the time domain waveform [19]–[22] are no longer reliable. Although techniques involving custom preamble design for NC-OFDM are available [23], they are not well suited to be applied in dynamic environments. This paper aims to solve this problem by designing a UCC to specifically aid timing and frequency offset recovery in addition to providing a low-rate communication link to share the control data.

We propose an independent UCC for each p2p link in the cognitive network that does not require any time synchronization with the other links in the network. Each such channel operates using the principles of direct sequence spread spectrum (DSSS) and is assigned a unique pseudo-noise (PN) sequence that is orthogonal to the other links' PN sequence. To address the dual-intent of the proposed UCC, the channel operates in one of two modes. The first mode is designed to aid timing and frequency offset recovery for NC-OFDM and the second mode is used to transmit control data. In the first mode, a two stage mechanism for timing and frequency offset recovery is proposed. The second mode uses straightforward spread spectrum techniques to transmit the control data. The underlay channel is always transmitted at noise floor so as to have minimal impact on the primary transmissions.

The proposed UCC is implemented on USRP N210 radios [24] with the GNU-Radio software platform [25] on the ORBIT testbed [26]. Experimental results are then used to explore the impact of the strength of the overlay transmissions and the choice of the various design parameters on the performance of the UCC. We study the performance of the proposed UCC in terms of the accuracy of timing and frequency offset estimation and the achievable data rate by varying the design parameters. In particular, experimental results indicate that the proposed design is capable of reliable timing and frequency offset recovery even in the presence of concurrent primary transmissions and supports about 10 to 20 kbps over a 1 MHz bandwidth at an uncoded symbol-error-rate of about 10^{-2} under typical operating conditions.

The remainder of this paper is organized as follows. We present our system model in Section II and discuss the design of the timing and frequency offset recovery mechanism in Section III. In Section IV we discuss our experimental setup and present the design choices and experimental results in Section V.

II. System Model

Consider a network of K p2p cognitive links operating over a total bandwidth of B, as shown in Fig. 1. Primary transmitters operate in certain parts of this bandwidth, thus fragmenting the available bandwidth into multiple noncontiguous segments. The primary transmissions are collectively denoted as $p(t)$. Each of the K p2p links is assumed to use NC-OFDM to access this fragmented spectrum and uses a total of N subcarriers. NC-OFDM restricts transmission to only a subset of these N subcarriers by first sensing the spectrum for incumbent transmissions and barring transmission over frequencies that are in use. Computing an optimal assignment of the available spectrum among the K links is a challenging problem [4], [27] and falls outside the scope of this work. We assume that a set of subcarriers $\mathcal{N}_i$ for $i = 1, 2, \ldots, K$ is assigned to each of the K links. As the bandwidth occupied by the incumbent transmissions changes, the spectrum assignment is recomputed and shared among the K links. The NC-OFDM signal transmitted by the kth transmitter is denoted as $s_k(t)$.

In addition to using NC-OFDM for data transfer, each of the K links is also supported by a p2p UCC, denoted as $c_k(t)$. This UCC is used to transmit the communication parameters, subcarrier assignment, and other control data to the receiver. Since the control channel plays a key role in enabling the use of NC-OFDM, it is important that this channel be easy to establish, while being robust to changes in the primary/secondary transmissions. A low-power UCC that spans the entire bandwidth, that is agnostic to spectrum assignment and has a minimal impact on primary transmissions is ideally suited for this purpose.

In such a setting, the received signal at the ith receiver of the cognitive network, without considering receiver impairments, is given by

$$r_i(t) = \underbrace{\sum_{k=1}^{K} h_k(t) * s_k(t)}_{K \text{ NC-OFDM signals}} + \underbrace{\sum_{k=1}^{K} h_k(t) * c_k(t)}_{K \text{ control signals}} + \underbrace{h_p(t) * p(t)}_{\text{primary signal}} + \underbrace{n(t)}_{\text{additive noise}}, \quad (1)$$

where the various components of the received signal are as labeled and $h_i(t)$ denotes the time domain channel impulse response. Note that the K NC-OFDM signals and the primary transmissions use orthogonal subcarriers and therefore do not interfere with each other.

A. NC-OFDM Signal Representation

The baseband representation of the NC-OFDM signal at the kth transmitter can be written as

$$s_k(t) = \sum_{l=0}^{\infty} \sum_{n \in \mathcal{N}_i} d_{kln}\ e^{j2\pi f_n (t - lT)} \text{rect}\Big(\tfrac{t - lT}{T}\Big), \quad (2)$$

where d_{kln} is the data symbol to be transmitted, f_n is the center frequency for the nth subcarrier, and rect$(\cdot)$ represents the rectangular function that is 1 in the unit interval and 0 elsewhere. T denotes the overall duration of one NC-OFDM signal, including the cyclic prefix. We assume that a cyclic prefix of length N_{cp} is used at each link. At the receiver, assuming a constant flat fading channel, after downconversion and accounting for frequency offset, the kth NC-OFDM signal can be represented as $h_k e^{j2\pi(\delta f_k)t} s_k(t)$, where h_k is the channel fading coefficient and δf_k is the frequency offset. When this signal is sampled at a rate of $1/T_s$, it can be written as

$$r_{i(s_k)}[m] = h_k e^{j2\pi(\delta f_k)(mT_s + \phi_k)} s_k(mT_s + \phi_k) \quad (3)$$

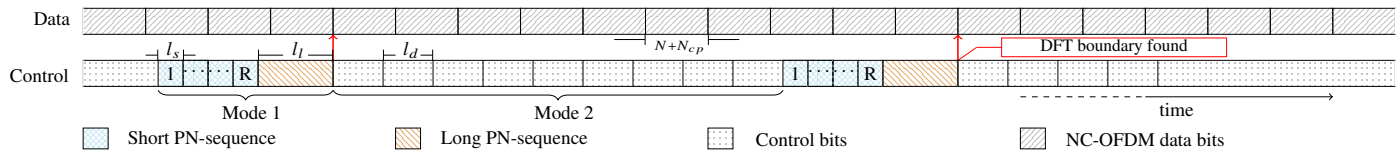

Fig. 2. Sequence of transmissions over the NC-OFDM-based data channel and the underlay control channel. Underlay control channel is used for timing and frequency offset recovery.

where $r_{i(s_k)}[m]$ denotes the contribution of $s_k(t)$ to the mth sample of $r_i(t)$, ϕ_k ($< T_s$) is the phase offset and (δf_k) is the frequency offset. Note that the K NC-OFDM signals are not assumed to be synchronized. We also assume that the sampling rate $T_s = T/(N + N_{cp}) = 1/B$.

The ith receiver decodes the NC-OFDM signal $s_i(t)$ from discrete time samples of the received signal $r_i(t)$. Two critical aspects of decoding an NC-OFDM signal are timing and frequency offset recovery. Timing recovery requires identifying the start of the NC-OFDM frames, which in the above representation occurs at every $(l(N + N_{cp}) + 1)$th sample. Frequency offset correction is also important to the reliable recovery of the NC-OFDM signals as it otherwise results in inter-carrier interference (ICI). Note that correcting the phase offset ϕ_i can be done at the detection stage using the aid of pilot symbols. While traditional OFDM-based systems use preambles that result in a time domain waveform with repeated patterns to aid timing and frequency recovery, the dynamic nature of spectrum allocation along with the presence of multiple concurrent transmissions make it difficult to directly apply these techniques to NC-OFDM-based systems. With these challenges in mind, we propose to use the UCC in a novel way to aid the timing and frequency offset recovery of the desired NC-OFDM signal. Details of the proposed mechanism are discussed in Section III.

B. Control Signal Representation

The low-power UCC is operated in one of two modes, as shown in Fig. 2. In mode 1, the channel is used to aid timing and frequency offset recovery and in mode 2, it is used to transmit control data. In mode 2, the control channel for each of K links operates as a conventional DS-CDMA channel where the message bits are first spread using a pre-assigned PN sequence $p_{kd}[m]$, of length l_d, and then transmitted over the air. The PN sequences for the K links are chosen to be orthogonal to each other so as to minimize multiple-access interference. The control signal can be represented as

$$c_k(t) = \sum_{l} \sum_{m=1}^{l_d} g_{kl} p_{kd}[m] \text{rect}\Big(\frac{t - l l_d T_c - (m-1)T_c}{T_c}\Big) \quad (4)$$

where T_c is the chip rate and g_{kl} is the control data to be transmitted. Since we assume that the UCC occupies the full bandwidth, we set $T_c = 1/B$, i.e., the sampling rate for the NC-OFDM signal and the control channel are the same. The UCC is always transmitted at a power equal to the noise floor in order to have minimal impact on the NC-OFDM signal. The receiver uses a single correlator and a demodulator to recover the transmitted control signals.

III. Control Channel Design for Timing and Frequency Offset Recovery

This section is focused on mode 1 of the control channel design. We propose a two-stage mechanism for timing and frequency offset recovery, as depicted in Fig. 2. In the first stage the ith transmitter transmits a short PN sequence $p_{is}[m]$ of length l_s repeatedly for R times. This is then followed by the transmission of a long PN sequence $p_{il}[m]$ of length l_l. The primary purpose of the first stage is to allow the receiver to compute an estimate of the frequency offset, while the second stage is used to identify the timing instance. At the ith receiver, suppose $r_i[m]$ denotes the samples of the received signal, the control channel component of interest in this sample during the first stage of mode 1, is given by

$$r_{i(c_i)}[m] = h_i p_{is}[1 + \text{mod}(m-1, l_s)] e^{j2\pi(\delta f_i)(mT_s + \phi_i)} \quad (5)$$

where we have assumed a flat fading channel. The receiver uses a correlator matched to $p_{is}[m]$ to serially scan the received signal to identify the transmission of the short PN sequence. The output of such a correlator is given by

$$w_{is}[m] = \sum_{n=1}^{l_s} r_i[m + n - l_s] p_{is}[n] \quad (6)$$

A short PN sequence is said to have been detected if $|w_{is}[m]|$ exceeds a certain threshold τ_s. Suppose in an ideal scenario, R such correlation peaks are detected, these R peaks can be used to compute a coarse estimate of the frequency offset. Let the indices corresponding to these R peaks be given by m, $m + l_s$, ..., $m + (R-1)l_s$. In a noiseless, interference less scenario and without any overlay NC-OFDM signals, two consecutive peaks differ only in phase by a value of

$$\Delta\psi = 2\pi(\delta f_i)((m + l_s)T_s + \phi_i) - 2\pi(\delta f_i)(mT_s - \phi_i) \quad (7)$$
$$= 2\pi l_s(\delta f_i)T_s, \quad (8)$$

This observation leads us to estimate the frequency offset as

$$\widehat{(\delta f_i)} = \frac{\sum_{n=1}^{R-1} \angle w_{is}[m + n l_l] - \angle w_{is}[m + (n-1)l_l]}{2\pi l_s T_s (R-1)} \quad (9)$$

It is however pertinent to address two key issues that emerge with regard to correlation peak detection. First, it is important that the length of the PN sequence l_s be small enough that $(\delta f_i) l_s T_s << 1$. When this condition is violated, the duration of the transmission of the PN sequence is such that its phase can undergo a rotation of more than 2π radians because of the frequency offset. This proves detrimental to the detection of the correlation peaks and also affects the accuracy of the offset estimate. This however brings up the second issue of being able to detect all R correlation peaks. Given the challenging environment under which this UCC is required

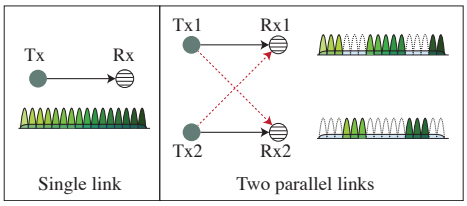

Fig. 3. Topologies used in experiments.

to operate and the necessity to limit the length l_s, we consider detecting only a fraction α of the peaks. This entails detecting αR peaks within a window of $l_s R$ samples, which then triggers the receiver to estimate the frequency offset and move to the next stage of timing recovery.

In the second stage, the receiver first uses the frequency offset estimate to correct the offset in the received signal, then puts this signal through a correlator matched to the long PN sequence $p_{il}[m]$. The output of this correlator is given by

$$w_{il}[m] = \sum_{n=1}^{l_l} e^{-j2\pi(\delta\hat{f}_i)(m+n-l_l)T_s} r_i[m+n-l_l] p_{il}[n] \quad (10)$$

A threshold τ_l is used to declare a correlation peak. When a peak is detected, it indicates the start of an NC-OFDM symbol. The use of a long PN sequence in the second stage ensures that even under challenging operating conditions, timing instances are reliably recovered and false peaks are minimized. Note that using the frequency offset estimate is crucial to enable the reliable detection of long PN sequences in the second stage.

A. Choice of Thresholds τ_l and τ_s

Under time varying conditions, the thresholds τ_l and τ_s cannot be held at fixed values and must instead be adaptive. To dynamically alter the threshold τ_l, we propose a first-order auto-regressive update procedure of the form

$$\tau_{l,new} = \beta \tau_{l,current} + \gamma \nu, \quad (11)$$

that updates the value of τ_l once every P samples (PT_s seconds), with the value of ν being either the latest long correlation peak detected in the previous PT_s seconds, or a preset value τ_o, in case no peaks were detected. The design parameters $0 \leq \beta \leq 1$, $0 \leq \gamma \leq 1$, and the integer P determine the rate at which the threshold adapts to current network conditions. In all our experiments we set $\beta = 0.7$ and $\gamma = 0.2$. A similar procedure can also be adopted for τ_s.

In the next two sections we discuss the implementation of the proposed UCC and the optimization of the various parameters involved in the design of the UCC.

IV. Experimental Setup

A. Topology

To test the performance of the proposed UCC, we perform a set of experiments on two particular network topologies, as shown in Fig. 3. In the single-link topology, the transmitter uses all available subcarriers to communicate with the receiver. In the two-link topology, the two links use two disjoint sets of subcarriers for communication. The UCC spans the whole bandwidth in both the cases. In the two-link topology, the control channels for the two links use orthogonal PN-sequences in both the modes. Note that from the UCC standpoint, the single-link topology is a more challenging environment to operate in than the two-link topology as the overlay interference in the two-link case gets split between two sources, with one being further away. Hence, we use results from the single-link topology as the basis for the choice of parameters for the UCC.

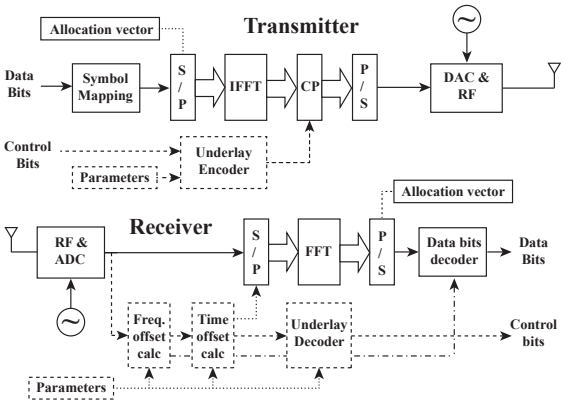

Fig. 4. Implementation of the transmitter and the receiver on USRP N210 radio nodes using GNU Radio.

B. Platform and Implementation

In our experiments the transmitter and receiver nodes shown in Fig. 3 are USRP N210 radio nodes [24], that are part of the larger ORBIT testbed [26]. The USRP N210 radios used in the experiment use the SBX transceiver daughter-card that can operate anywhere from 400 MHz to 4.4 GHz, provide a maximum bandwidth of 40 MHz and transmit up to 100 mW of power. GNU Radio is a free and open-source SDR framework that provides the application programming interface (API) for several hardware platforms, including many USRP devices [25]. The NC-OFDM data paths and the corresponding UCC paths are implemented in C++ and Python in GNU Radio. Fig. 4 shows the block diagram of the transmitter and receiver in our experimental setup. All the necessary parameters for the configuration are provided to the transmitter and receiver by an outside controller. The transmit chain has a control path that runs parallel to the data path, however, since the control also aids timing recovery, the two paths are merged at the block where cyclic prefix is added to the NC-OFDM signal.

At the receiver, the incoming stream of symbols is used as input to two parallel chains. The first chain is used for timing recovery, frequency offset estimation, and decoding of control data as described in Section II-B, while the second chain is used to decode the NC-OFDM signal. We use the adaptive thresholding procedure outlined in Section III-A to set the threshold for the long correlation while using a small, fixed threshold to identify short correlation peaks.

C. Transmission Parameters

In all the experiments the UCC's power is set to be at noise floor i.e., underlay-to-noise-ratio (UCNR) = 0 dB, while the transmit overlay-signal-to-noise ratio (OSNR) is varied from 4 to 10 dB. Experiments are conducted to study (a) the accuracy

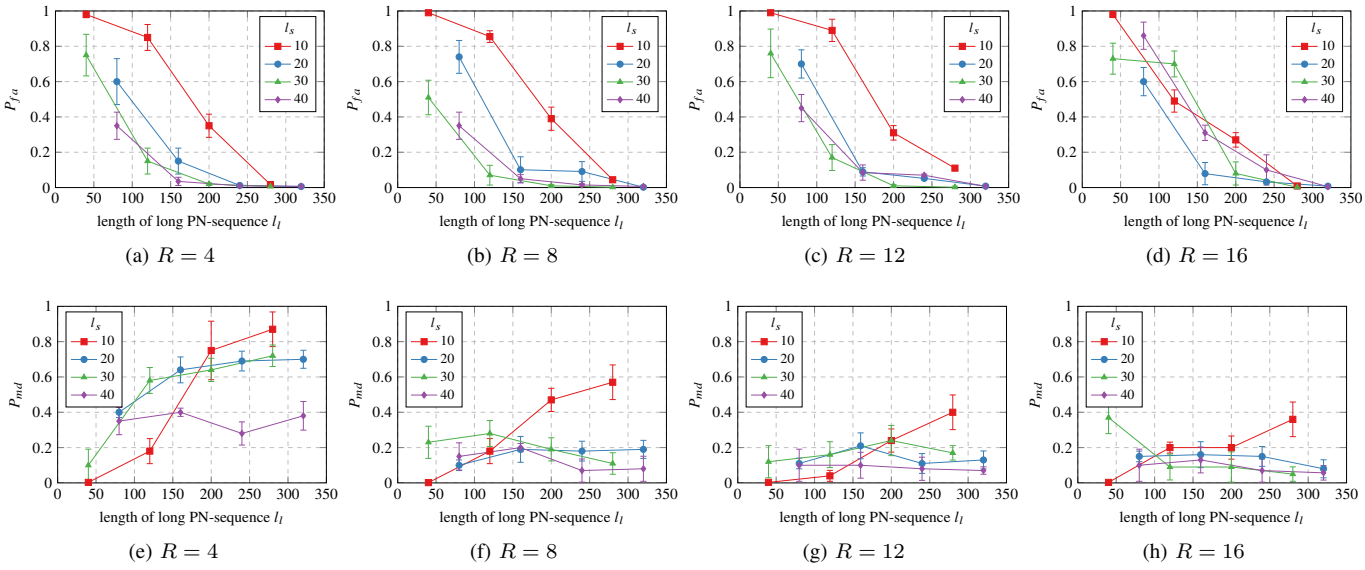

(a) $R = 4$ (b) $R = 8$ (c) $R = 12$ (d) $R = 16$

(e) $R = 4$ (f) $R = 8$ (g) $R = 12$ (h) $R = 16$

Fig. 5. Probability of false alarm P_{fa} and probability of missed detection P_{md} for various combinations of the parameters l_s, l_l and R.

of the timing offset estimation and (b) the symbol error rate (SER) of the UCC as a function of the strength of the overlay NC-OFDM signal. The various design parameters involved in the UCC are designed assuming a transmit OSNR of 10 dB.

In all experiments, we use a 1 MHz bandwidth and divide this bandwidth between $N = 64$ subcarriers. We set the cyclic prefix length to be $N_{cp} = 16$, resulting in a total NC-OFDM symbol length of $N + N_{cp} = 80$. For the two-link topology, subcarriers 1–15 and 34–48 are assigned to link 1, subcarriers 17–31 and 50–64 are assigned to link 2 and subcarriers 16, 32, 33 and 49 are used as guard bands. The NC-OFDM subcarriers are modulated using the QPSK constellation and the control data using BPSK. Timing and frequency offset recovery is only performed periodically, after the transmission of multiple NC-OFDM symbols, we thus ensure that $l_l + Rl_s + Vl_d$ is an integer multiple of 80, where V is the number of control data symbols transmitted in mode 2. To analyze the performance of the timing and frequency offset estimation we vary the values of l_s, l_l and R, while keeping all other parameters constant. Similarly, to calculate the bit error rate for UCC we vary the value of l_d and transmit OSNR while keeping UCNR at 0 dB and all other parameters constant.

V. Results and Discussion

The first set of experiments aims to study the impact of the parameters l_s, l_l and R on the accuracy of timing and frequency offset recovery. We use the single-link topology for this purpose. Fig. 5 shows the results of such an experiment where the performance of UCC is measured in terms of the probability of missing a timing instant and the probability of reporting a false timing instant. Figs. 5a to 5d show the probability of false alarm P_{fa}, while Figs. 5e to 5h show the probability of missed detection P_{md} for different values of l_s, l_l and R. In all these figures, l_s is chosen from the set $\{10, 20, 30, 40\}$ while the value of l_l is varied between 40 to 320. Focusing on Fig. 5a and Fig. 5e, we see that although P_{fa} decreases with increasing l_l, setting $R = 4$ is insufficient to bring P_{md} to within a reasonable range. A large P_{md} for large values of l_l suggests that a reliable estimate of the frequency offset is difficult to obtain for small values of R. In general it can be noticed that $R \geq 8$ is required to keep both P_{fa} and P_{md} to within acceptable levels. Note also that in Figs. 5a-5d, P_{fa} appears to increase with R. Although this appears counterintuitive, this can be explained by noting that for small values of R, P_{md} is so high that very few peaks are detected, leading to a low value for P_{fa}. For $R \geq 8$, it is seen that as the value of l_l increases both P_{fa} and P_{md} decrease. Based on these observations, it appears that setting $l_s = 40$, $l_l = 320$ and $R = 8$ provides a good trade-off between reliable timing and frequency offset recovery and transmit overhead incurred in operating the UCC in mode 1 instead of mode 2. We henceforth use these parameter settings for the remaining experiments.

The next set of experiments is performed to measure the SER of the UCC in the presence of overlay NC-OFDM signal. Towards this end, we hold UCNR at 0 dB and vary the transmit OSNR between 0 to 10 dB. All parameters are held constant except for the spreading code length l_d which is chosen from the set $\{20, 40, 60\}$. We conduct these experiments for both single link and two-link topology of Fig. 3. Figs. 6a and 6b show the results from these experiments where Fig. 6a shows the SER for the single link topology and Fig. 6b shows the SER over the two links in the two-link topology. We see that overall SER performance is comparable for both topologies. For lower values of transmit OSNR the two-link topology actually performs better as the received OSNR is slightly lesser in the two-link case due to difference in the distances to the two transmitters. It is seen that it is possible to achieve an uncoded SER of 10^{-2} even when the transmit OSNR is up to 6-8 dB with $l_d = 60$. Note that these error rates include errors due to false alarms in the timing recovery stage. SER can be further reduced by using a phase-locked loop to improve the accuracy of the timing recovery mechanism. Under the current parameter settings this translates to a symbol rate of 11 kbps over 1 MHz channel, assuming the duration of mode 2 is twice the duration of mode 1.

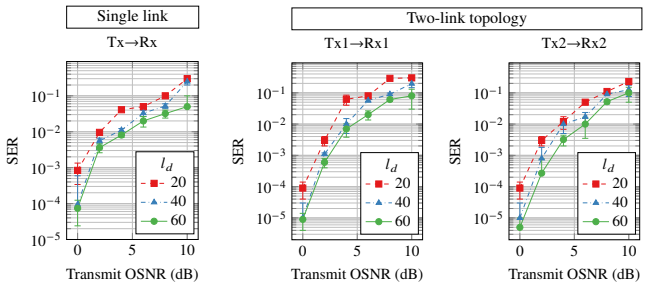

Fig. 6. SER of UCC as the transmit OSNR is varied. Errors due to false alarms in timing recovery are also counted.

VI. Conclusion

This paper considered the design of an underlay control channel for a cognitive network consisting of multiple NC-OFDM-based p2p links that operate over a wide bandwidth consisting of multiple disjoint bands. In addition to sharing control data, the proposed underlay control channel based on DSSS transmission is also used for timing and frequency recovery of NC-OFDM transmissions. The control channel operates in one of two modes. The first mode aids timing and frequency recovery through a two-step process, while the second mode is used for control data transmission. Such a control channel was implemented on USRPs in the ORBIT testbed using GNU Radio. Experimental results reveal that such a channel can be relied upon for robust timing and frequency offset recovery while supporting 10 to 20kbps over a 1 MHz bandwidth at an uncoded symbol-error-rate of about 10^{-2} under typical operating conditions.

Acknowledgment

This work is supported in part by a grant from the U.S. Office of Naval Research (ONR) under grant number N00014-15-1-2168. The work of S. Kompella is supported directly by the Office of Naval Research.

References

[1] R. Rajbanshi, A. M. Wyglinski, and G. J. Minden, "An efficient implementation of NC-OFDM transceivers for cognitive radios," in *Proc. EAI Int. Conf. on Cognitive Radio Oriented Wireless Netw. and Commun. (CROWNCOM)*, Jun. 2006.

[2] J. D. Poston and W. D. Horne, "Discontiguous OFDM considerations for dynamic spectrum access in idle TV channels," in *Proc. IEEE Symp. on New Frontiers in Dynamic Spectrum Access Networks (DySPAN)*, 2005, pp. 607–610.

[3] R. Kumbhkar, M. N. Islam, N. B. Mandayam, and I. Seskar, "Rate optimal design of a wireless backhaul network using TV white space," in *Proc IEEE Int. Conf. Commun. Syst. Networks (COMSNETS)*, Jan. 2015.

[4] R. Kumbhkar, T. Kuber, G. Sridharan, N. B. Mandayam, and I. Seskar, "Opportunistic spectrum allocation for max-min rate in NC-OFDMA," in *Proc. IEEE Symp. on New Frontiers in Dynamic Spectrum Access Networks (DySPAN)*, Sep. 2015, pp. 385–391.

[5] B. F. Lo, "A survey of common control channel design in cognitive radio networks," *Elsevier Physical Communication*, vol. 4, no. 1, pp. 26–39, 2011.

[6] M. E. Sahin and H. Arslan, "System design for cognitive radio communications," in *Proc. IEEE Int. Conf. Cognitive Radio Oriented Wireless Networks Commun.*, 2006.

[7] D. L. Wasden, H. Moradi, and B. Farhang-Boroujeny, "Design and implementation of an underlay control channel for cognitive radios," *IEEE J. Sel. Areas Commun.*, vol. 30, no. 10, pp. 1875–1889, Nov. 2012.

[8] R.-R. Chen, K. H. Teo, and B. Farhang-Boroujeny, "Random access protocols for collaborative spectrum sensing in multi-band cognitive radio networks," *IEEE J. Sel. Topics Signal Process.*, vol. 5, no. 1, pp. 124–136, 2011.

[9] K. Bian, J.-M. Park, and R. Chen, "A quorum-based framework for establishing control channels in dynamic spectrum access networks," in *Proc. ACM Annual Int. Conf. on Mobile Computing and Netw. (MobiCom)*, 2009, pp. 25–36.

[10] C. Cormio and K. R. Chowdhury, "Common control channel design for cognitive radio wireless ad hoc networks using adaptive frequency hopping," *Elsevier Ad Hoc Networks*, vol. 8, no. 4, pp. 430–438, 2010.

[11] B. F. Lo, I. F. Akyildiz, and A. M. Al-Dhelaan, "Efficient recovery control channel design in cognitive radio ad hoc networks," *IEEE Trans. Veh. Technol.*, vol. 59, no. 9, pp. 4513–4526, Nov. 2010.

[12] M. Petracca, R. Pomposini, F. Mazzenga, R. Giuliano, and M. Vari, "An always available control channel for cooperative sensing in cognitive radio networks," in *Proc. IEEE IFIP Wireless Days Conf.*, 2010.

[13] D. Li, X. Dai, and H. Zhang, "Sidelobe suppression in NC-OFDM systems using constellation adjustment," *IEEE Commun. Lett.*, vol. 13, no. 5, pp. 327–329, May 2009.

[14] A. Ghassemi, L. Lampe, A. Attar, and T. Gulliver, "Joint sidelobe and peak power reduction in OFDM-based cognitive radio," in *Proc. IEEE Veh. Technol. Conf. (Fall)*, Sep. 2010.

[15] A. Dutta, D. Saha, D. Grunwald, and D. Sicker, "Practical implementation of blind synchronization in NC-OFDM based cognitive radio networks," in *Proc. ACM Workshop Cognitive Radio networks*, 2010.

[16] J. Acharya, H. Viswanathan, and S. Venkatesan, "Timing acquisition for non contiguous OFDM based dynamic spectrum access," in *Proc. IEEE Symp. on New Frontiers in Dynamic Spectrum Access Networks (DySPAN)*, Oct. 2008.

[17] B. Huang, J. Wang, W. Tang, and S. Li, "An effective synchronization scheme for NC-OFDM systems in cognitive radio context," in *Proc. IEEE Symp. on New Frontiers in Dynamic Spectrum Access Networks (DySPAN)*, Sep. 2010.

[18] D. Qu, J. Ding, T. Jiang, and X. Sun, "Detection of non-contiguous OFDM symbols for cognitive radio systems without out-of-band spectrum synchronization," *IEEE Trans. Wireless Commun.*, vol. 10, no. 2, pp. 693–701, Feb. 2011.

[19] T. Schmidl and D. Cox, "Robust frequency and timing synchronization for ofdm," *IEEE Trans. Commun.*, vol. 45, no. 12, pp. 1613–1621, Dec. 1997.

[20] H. Minn, V. Bhargava, and K. Letaief, "A robust timing and frequency synchronization for OFDM systems," *IEEE Trans. Wireless Commun.*, vol. 2, no. 4, pp. 822–839, Jul. 2003.

[21] M. Morelli, C.-C. Kuo, and M.-O. Pun, "Synchronization techniques for orthogonal frequency division multiple access (OFDMA): A tutorial review," *Proc. IEEE*, vol. 95, no. 7, pp. 1394–1427, Jul. 2007.

[22] B. Ai, Z.-X. Yang, C.-Y. Pan, J. hua Ge, Y. Wang, and Z. Lu, "On the synchronization techniques for wireless OFDM systems," *IEEE Trans. Broadcast.*, vol. 52, no. 2, pp. 236–244, June 2006.

[23] S. Feng, H. Zheng, H. Wang, J. Liu, and P. Zhang, "Preamble design for non-contiguous spectrum usage in cognitive radio networks," in *Proc. IEEE Wireless Commun. Netw. Conf. (WCNC)*, Apr. 2009.

[24] USRP software radio systems: Ettus Resarch. [Online]. Available: http://www.ettus.com/

[25] GNU Radio Website, accessed February 2012. [Online]. Available: http://www.gnuradio.org

[26] WINLAB, Rutgers, The State University of New Jersey. ORBIT: Open access research testbed for next-generation wireless networks. [Online]. Available: http://www.orbit-lab.org

[27] M. N. Islam, N. B. Mandayam, S. Kompella, and I. Seskar. (2013) Power optimal non-contiguous spectrum access. [Online]. Available: http://arxiv.org/abs/1309.0861